Thermoelectric properties of the degenerate Hubbard model

V. S. Oudovenko* and G. Kotliar
Serin Physics Laboratory, Rutgers University, 136 Frelinghuysen Road, Piscataway, New Jersey 08854
(Received 11 December 2000; revised manuscript received 9 August 2001; published 17 January 2002)

We investigate the thermoelectric properties of a system near a pressure-driven Mott-Hubbard transition. The dependence of the thermopower and the figure of merit on pressure and temperature within a degenerate Hubbard model for integer filling $n=1$ is calculated using dynamical mean-field theory. The quantum Monte Carlo method is used to solve the impurity model. Obtained results can qualitatively explain thermoelectric properties of various strongly correlated materials.

DOI: 10.1103/PhysRevB.65.075102 PACS number(s): 72.15.Jf, 75.20.Hr, 71.10.Fd

The discovery of strongly correlated materials and improvement in theoretical methods offer perspectives in the search for systems with good thermoelectric performance.[1] The dimensionless figure of merit, $ZT=S^2\sigma T/\kappa$, provides us with a quantified measure of the thermoelectric performance of materials. Higher values of the thermoelectric figure of merit corresponds to better thermoelectric properties. To get maximal thermoelectric response at a fixed temperature, T, we need to have maximum possible thermopower, S, and the electrical conductivity, σ, while the thermal conductivity, κ, should be the smallest possible. The thermal conductivity has two contributions, an electronic, κ_e, and lattice, κ_L, one; $\kappa=\kappa_e+\kappa_L$. For some time, the highest value of the figure of merit has been equal to 1 and little improvement in getting materials with higher figures of merit has been achieved in the last two decades. Since the electronic structure of strongly correlated electron systems exhibit properties which have no analogy to those of weakly correlated compounds, it is important to understand their physical properties and how they impact the thermoelectric power. Strongly correlated electrons are sensitive to small changes in their control parameters such as temperature, doping, and pressure and hence require a detailed investigation. There is now a strong interest in understanding how these changes affect the thermoelectric properties in order to find more efficient material with higher thermoelectric response. Even a modest increase in ZT could substantially impact a number of applications.[1]

Two important parameters in strongly correlated electron systems are the carrier concentration and the ratio of the on-site interaction U to the bandwidth W. This ratio can be altered by applying external pressure or internal pressure by means of isovalent substitutions.

In this paper we study behavior of the figure of merit and the thermopower near a pressure-driven metal-insulator transition (MIT) within the framework of the degenerate Hubbard model. Our focus is on the effects of orbital degeneracy. There are several motivations for our study. First, in many strongly correlated materials, the orbitals, which bring a major contribution to unusual physical properties, are degenerate. Second, the orbital degeneracy allows us to study the effects of particle-hole asymmetry in the Mott insulating state with filling $n=1$ in a natural way (one can also introduce particle-hole asymmetry in this case by adding hopping integrals beyond nearest neighbors). Third, the degeneracy will allow us to use the integer filling $n=1$ that in the real system corresponds to the situation in which the number of electrons is equal to the number of sites. We use Coulomb repulsion U and temperature T as the parameters to vary and take the half bandwidth D to be unity.

While calculation of the numerical value of the thermoelectric coefficient requires detailed modeling of the band structure and interaction constants of the relevant compounds, we expect that the *qualitative* features related to the thermoelectricity of a Mott insulator at integer filling can be captured by the simplest model, the degenerate Hubbard model, and we undertake this study in the paper. Indeed the trends discussed here are found in $NiS_{2-x}Se_x$ and $Ni_{1-x}Co_xS_2$, as we discuss toward the end of this paper. The algorithms necessary for more realistic calculations of thermoelectricity will be discussed in a future publication.[2]

To treat the two-band degenerate Hubbard model we use dynamical mean-field theory (DMFT).[3] Recent development of DMFT has given a boost to the study of strongly correlated systems and their properties. In particular it has resulted in a detailed understanding of the Mott transition.

Previous studies of thermoelectric properties using DMFT were done within the framework of the one-band Hubbard model;[4–6] strong temperature and doping dependence of the thermopower was reported. Pálsson and Kotliar considered the orbital degeneracy away from half filling in the limit of infinite interaction strength.[7] A good description of the Seebeck coefficient dependence on temperature and doping for titanates was obtained.

In this paper we focus on the integer occupancy case with orbital degeneracy. We also keep U finite and study dependence of thermoelectric properties on the interaction. Changing the ratio of the interaction strength, one can mimic the effects of pressure.

The N-fold degenerate Hubbard Hamiltonian reads

$$H=-\sum_{\langle ij\rangle,\sigma} t_{ij}c^{\dagger}_{i\sigma}c_{j\sigma}+\frac{U}{2}\sum_{i,\sigma\neq\sigma'} n_{i\sigma}n_{i\sigma'}-\mu\sum_{i,\sigma} n_{i\sigma}, \tag{1}$$

where $\langle ij\rangle$ runs over nearest-neighbor sites, and σ is the spin and orbital indices which run from 1 to N. The two-band degenerate Hubbard model corresponds to $N=4$. The hopping matrix is given by t_{ij}, U is the Coulomb repulsion, and μ is the chemical potential. We also want to restrict ourselves to the paramagnetic phase (in both spin and orbit in-

dices), i.e., we are interesting in the metal-insulator transition and its influence on transport properties due to electronic correlations only. It is worth mentioning that orbital degeneracy suppresses the magnetic correlations enough to make our assumption easily fulfilled.[8] To make computations still easier we assume $t_{ij}=t$.

In this paper we use the model on a cubic lattice. For calculation of thermodynamic properties we use the semicircular density of states (DOS) $\rho(\epsilon)=(2/\pi D)\sqrt{1-(\epsilon/D)^2}$, with the half bandwidth $D=W/2=2t$. The semicircular DOS corresponds to an infinite coordination Bethe lattice which, as it was found earlier,[3] gives a good description of three-dimensional systems.

The next step is to solve the Hubbard model. The standard way in DMFT to do this is to map the lattice Hubbard model onto the effective impurity problem, which is a generalized single impurity Anderson model, where the operators carry an orbital index. Supplementing with the self-consistency condition[3] solution of the impurity model gives us the solution of the original Hubbard model. The quantum Monte Carlo (QMC) method with an extended Hirsch-Fye algorithm[9,10] is used as the impurity solver. To reduce computational errors (the Trotter breakup) the imaginary-time interval is set to $\Delta\tau=1/4$. During the self-consistency procedure one needs to make direct and inverse Fourier transformations for the Green's functions (GF's). In the present calculations we use a modified Fourier transformation in order to get correct results (for details, see the Appendix).

The output of the self-consistent procedure described above is the Green's function on an imaginary-time axis. To calculate the thermoelectric properties we need to know the behavior of the GF's on the real frequency axis. The maximum entropy method is used to make the analytical continuation of the imaginary-time GF's to the DOS on the real frequency axis. Knowing the imaginary part of the GF we reconstruct frequency dependence of the real part $G(\omega)$ through Kramers-Kronig relations. The obtained GF is used to calculate the transport coefficients.

Using Kubo formalism one can express thermoelectric coefficients in terms of current-current correlation functions which are reduced within DMFT to averages over the spectral density function $\rho(\epsilon,\omega)$:[7,11]

$$S=-\frac{A_1}{eA_0},\quad \sigma=\frac{e^2}{T}A_0,\quad \kappa=\left(A_2-\frac{A_1^2}{A_0}\right), \tag{2}$$

where the coefficients A_n have the following form,

$$A_n=\frac{1}{V}\sum_{k,s}\int d\omega\rho_s^2(k,\omega)\left(\frac{\partial\epsilon_k}{\partial k_x}\right)^2\left(-T\frac{\partial f(\omega)}{\partial\omega}\right)(\beta\omega)^n$$

$$=N_{deg}\pi\int_{-\infty}^{\infty}d\omega d\varepsilon\frac{\rho^2(\varepsilon,\omega)(\omega\beta)^n}{4\cosh^2\left(\frac{\beta\omega}{2}\right)}\Phi(\varepsilon), \tag{3}$$

where T is temperature, $f(\omega)$ is the Fermi distribution function, and s describes spin and orbital indices which run from 1 to N_{deg}. The spectral density, $\rho_s(k,\omega)$, and the transport function, $\Phi(\varepsilon)$, contain the relevant information about the bare band structure, ϵ_k:

$$\Phi(\varepsilon)=\frac{1}{V}\sum_k\left(\frac{\partial\epsilon_k}{\partial k_x}\right)^2\delta(\varepsilon-\epsilon_k). \tag{4}$$

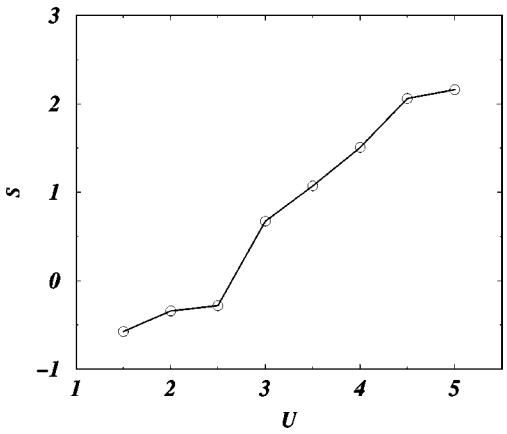

FIG. 1. Dependence of the thermopower S (in units of $k_B/e=86\ \mu$V/K) on Coulomb interaction U (in $D=1$ eV) for $\beta=8$.

As is seen from the above formulas (3) and (4), contribution to the thermopower strongly depends on temperature. For low temperatures only states close to the Fermi surface contribute to thermoelectric properties while for high temperatures the entire Brillouin zone is important. Coulomb repulsion, U, acts on the transport coefficients via changes in the spectral density function, $\rho(\varepsilon,\omega)$. There is a very simple mnemonic rule to define the sign of the thermopower. For small temperatures it depends on the DOS slope at the Fermi energy: if the DOS curve rises when it crosses the Fermi energy then the sign is negative and vice versa. For very high temperatures it depends on the weight of the Hubbard bands: if the weight of the Hubbard band above the Fermi energy is larger than the contribution from the band below the Fermi level then the thermopower is negative. This rule will help us easily understand the thermopower behavior analyzing the temperature dependence of the DOS.

In Fig. 1 we plot dependence of the thermopower on interaction strength U. The thermopower changes sign in a region of Coulomb repulsion $2.5<U<3$, the region where the system undergoes a metal-insulator transition at low temperatures. The MIT for high temperatures transforms into the metal-insulator crossover that is reflected in the spectral function (DOS) behavior presented in Fig. 2. It is worth noticing the quite strong S dependence on U in that crossover region. When $U\to 0$ the thermopower will have a finite value depending on temperature, and in the opposite limit $U\to\infty$ we expect saturation of the thermopower dependence which will also be temperature dependent. The interaction dependence of the thermopower helps us qualitatively understand the pressure influence onto the system as well as behavior of a system (e.g., $NiS_{2-x}Se_x$) changing its properties from insulating to metallic by varying the bandwidth. It follows from the fact that the only important parameter in the system

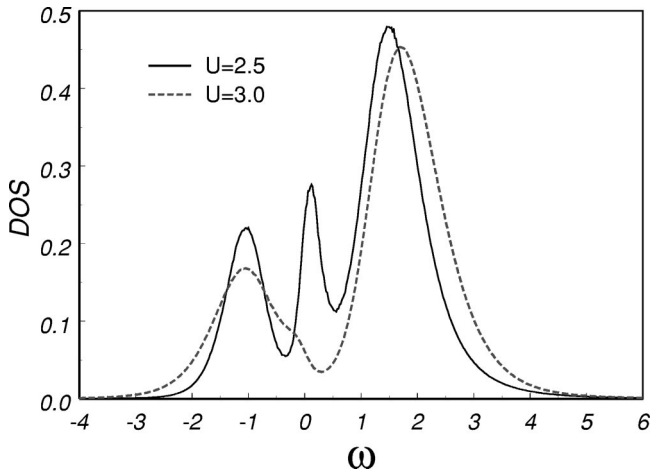

FIG. 2. Spectral functions (DOS) for $U=2.5$ and 3 for $\beta=8$.

is the ratio U/W and one can vary any of the two variables to get a qualitative description of the system's properties.

Behavior of the figure of merit on interaction strength (Fig. 3) is possible to understand from its definition. It is minimum where the thermopower changes sign. After the sign changes it substantially increases and is maximum for higher values of U. Rather high values of ZT (more than 1) can be explained by the absence of the lattice contribution in the thermal conductivity. If one takes into account the lattice thermal conductivity the figure of merit drops to a value below 1. Usual values of the lattice contribution to the thermal conductivity in transition-metal oxides lay in the region 0.1–10 W/mK. We believe that 1 W/mK is a reasonable value for pyrites. We see that the figure of merit is maximal for interaction U between 4 and 4.5, but even in this region, the obtained figure of merit could not compete with the one for semiconductors due to the lattice contribution to the thermal conductivity.

Temperature dependence of the thermopower for $U=3$ presented in Fig. 4 can be easily explained from analysis of the DOS temperature dependence in Fig. 5. For very low temperatures the thermopower has linear dependence (one

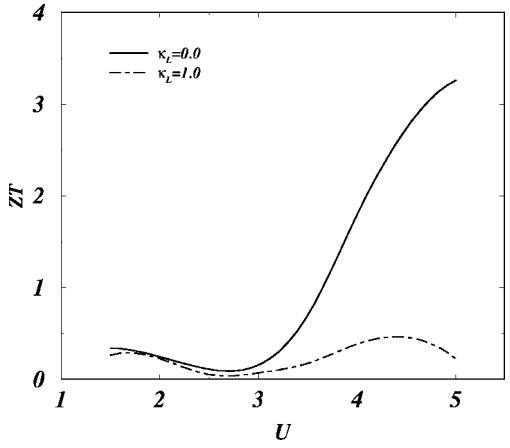

FIG. 3. The figure of merit, ZT, vs interaction strength, U, for temperature $\beta=8$ and different values of the lattice conductivity κ_L [W/mK].

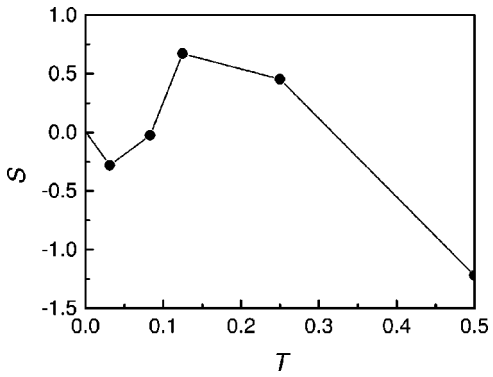

FIG. 4. Temperature dependence of the thermopower S for $U=3$. The solid line is a guide for the eye.

can show it analytically; it is nearly impossible at the present stage to reach very low temperatures with the QMC method) and a negative sign indicating the presence of quasiparticles in the system, which is clearly seen in Fig. 5 ($\beta=16$) where a good quasiparticle peak in the Fermi energy is observable. With increasing temperature a smooth crossover from quasiparticle excitations to incoherent ones is reflected in nonmonotonic thermopower dependence which changes sign from negative to positive. In Fig. 5 for temperatures $\beta=12$ and $\beta=8$ we see how the quasiparticle peak of the DOS gets lower and then disappears. From this observation we can conclude that a positive value of S tells us that the band structure consists of two Hubbard subbands only. Similar behavior of the thermopower (with the sign change) occurs in the single-band Hubbard model upon doping[11] and in the Hubbard model with frustration[6] as well as in the periodic Anderson model.[12] Further temperature behavior of the thermopower is new, to our best knowledge. At a temperature $\beta=8$ in Fig. 4 the thermopower reaches its maximum and then starts decreasing (we should notice here that temperature $\beta=4$ is the coherent temperature for the studied system). For $\beta=4$ the spectral function consists of two bands, one of which is a lower Hubbard band, which is closer to the Fermi energy and gives a greater contribution to the thermopower than does the upper one, which is located a bit further from the chemical-potential position. With increasing temperature the two bands become less asymmetric to the Fermi energy and the weight from the upper Hubbard band ($n=1$) becomes larger than the contribution from the lower band. This means that the thermopower should became negative, as is seen in Fig. 4 (the last point). And finally, for very high temperature the two bands collapse into one. But the sign of the thermopower remains unchanged for the same reason as discussed above. The thermopower sign change in the high-temperature limit due to the Mott-Hubbard bands' collapse was reported in Ref. 13.

To gain further understanding of the temperature and interaction dependencies of the thermopower we study its high-frequency behavior in the high-temperature limit. To do so we generalize the thermoelectric response to finite frequencies (ac thermopower):[14]

$$S(\omega)=-\frac{1}{eT}\frac{L^{12}(\omega)}{L^{11}(\omega)}, \tag{5}$$

where coefficients L^{11} and L^{12} are defined as

$$L_{ji}^{1n}(\omega)=\frac{ie^{\beta\Omega}}{\omega\beta}\sum_{\mu\nu}\frac{\langle\mu|q_i|\nu\rangle\langle\nu|J_j^n|\mu\rangle(e^{-\beta\varepsilon_\mu}-e^{-\beta\varepsilon_\nu})}{\omega+\varepsilon_\mu-\varepsilon_\nu+i\delta}.$$

Here $e^{-\beta\Omega}=\mathrm{Tr}(e^{-\beta(H-\mu N)})$, $i,j=x$, $J_x^1=j_x$, $J_x^2=j_x^Q$, j_x and j_x^Q are electrical and heat currents in the x direction, correspondingly, and q_x is the polarization operator satisfying $j_x(t)=\partial q_x(t)/\partial t$.

Expanding the numerator and denominator of the thermopower [$L^{11}(\omega)$ and $L^{12}(\omega)$] in frequency and dividing one onto the other we obtain the following expansion of the thermopower in the high-frequency limit:

$$S(\omega)=-\frac{\beta}{e}\left(\frac{\langle[q_x,j_x^Q]\rangle}{\langle[q_x,j_x]\rangle}+\mathcal{O}(\omega)\right). \tag{6}$$

The relevant commutators are given by

$$-\frac{1}{it}[q_x,j_x^Q]=\sum_{js}\left\{t[c_{j+2x}^\dagger c_{js}+c_{j-2x,s}^\dagger c_{j,s}]+\mu[c_{j+x,s}^\dagger c_{j,s}+c_{j-x,s}^\dagger c_{j,s}]-U\left[c_{j+x,s}^\dagger c_{j,s}\sum_{s'\neq s}n_{j+xs'}+c_{j-x,s}^\dagger c_{j,s}\sum_{s'\neq s}n_{j-xs'}\right]\right\}. \tag{7}$$

This expression consists of three terms. The first one, proportional to t, does not contribute to the high-temperature expansion if one takes into account only nearest-neighbor hoppings. The second term (proportional to the chemical potential) is similar to what we have in the denominator and the last one proportional to U contributes to the high-temperature expansion of the thermopower. The final result is presented below:

$$S(\omega)\overset{T\to\infty}{\to}-\frac{\beta}{e}\left(-\mu+U\frac{\overline{n}}{1-n}\right), \tag{8}$$

where $\overline{n}$ corresponds to the contribution to filling n coming from $N_{deg}-1$ degrees of freedom (spin and orbital) and is equal to $\Sigma_{\sigma,\sigma'\neq\sigma}\langle(1-n_\sigma)n_{\sigma'}\rangle$. If one assumes high-temperature behavior of the chemical potential in the form $\mu/T=\alpha$, where α should be negative for the filling $n<\frac{1}{2}N_{deg}$, one obtains that the sign of the thermopower should be negative in the high-temperature limit. Hence ac and dc thermopowers have the same sign in the high-temperature limit.

It is quite difficult to make a direct comparison of a model calculation and situation in real materials due to complexity and the wide variety of real structures. To make a comparison with our model calculations we need a material with a degenerate e_g band hosting one electron (hole). As we mentioned in the introduction good candidates for the comparison are pyrite compounds with doubly degenerate $3d-e_g$ Ni bands. An attempt to understand high-temperature dependence of the thermopower in these materials on the basis of one-band electron correlation theory with a good fit of experimental data using a six-parameter model was given some years ago in the work of Kwizera *et al.*[15] To explain low-temperature dependence of the thermopower it was suggested that both holes and electrons participate in charge transport and a two-band model was proposed as an appropriate model for data interpretation.[13] Our calculations show that the two-band degenerate Hubbard model treated within DMFT is a sufficient model for at least a qualitative description of pyrites in the whole temperature range.[13,15,16] In the case of the half-filled Ni $3d-e_g$ band in the $NiS_{2-x}Se_x$ theoretical model under consideration, due to the symmetry in the system, it should give zero thermopower for all temperatures, while experimentally it is zero only for temperature $T<100$ K. For higher temperatures the thermopower becomes positive. It is clear that one needs to take into account effects of other bands (filled t_{2g} band in the first turn). The thermopower behavior in $Ni_{1-x}Co_xS_2$ with temperature looks rather similar to $NiS_{2-x}Se_x$, but with Co substitution of Ni atoms, occupancy of the $3d-e_g$ band changes from two ($x=0$) to one ($x=1$). One can track the experimental situation in $NiS_{2-x}Se_x$ by analyzing model calculations (for temperatures low enough to neglect contributions coming from other bands) especially in the case of CoS_2, which corresponds to a one-quarter filled $3d-e_g$ band.

In conclusion, we calculated dependencies of the thermopower and the figure of merit on interaction strength and temperature of the thermopower in the two-band degenerate Hubbard model for integer filling $n=1$. The strong dependence on studied parameters was obtained. Analytical estimations of the high-frequency limit of ac thermopower is provided. In the high-temperature limit ac and dc thermopowers have the same sign (negative for filling $n<0.5$). We expect that the thermopower behavior in the three-band degenerate Hubbard model would behave in a similar way. This means that we can qualitatively understand the behavior of the thermoelectric properties in a wide range of strongly correlated materials where a major role is played by *d*- and *f*-shell electrons.

Systems near the temperature-driven Mott transition exhibit very rich thermoelectric behavior. As we cross the localization-delocalization threshold the thermopower increases substantially. The high-temperature precursors of the first-order Mott transition takes place at lower temperature. As the temperature is lowered, and the critical Mott endpoint is approached, the specific heat diverges and the entropy jumps. The figure of merit is low in this crossover regime because of the great deal of cancellation between the quasiparticle contributions which are, in our model, electronlike, and the Hubbard band contributions which are holelike. A detailed phase diagram temperature versus filling for different values of U using the current approach will be studied elsewhere.

The authors are indebted to G. Pálsson, and A. I. Lichtenstein for many helpful and stimulating discussions. We also acknowledge usage of the Rutgers Computational Grid PC cluster as well as the NERSC Cray T3E supercomputer which made our computations possible. The research was

supported by the American Chemical Society Petroleum Research Fund, Grant No. ACS-PRF 33495-ACS.

APPENDIX: FOURIER TRANSFORMATION IN QMC CALCULATIONS

In the self-consistent procedure to solve the impurity problem using the QMC method[3] we need to do two direct Fourier transformations for GF's $G(\tau)$ and $G_0(\tau)$ (the Weiss function) and one inverse Fourier transformation for $G_0(\tau)$ only. Function $G_0(\tau)$ is an input for QMC simulations producing $G(\tau)$. Two direct Fourier transformations are necessary to impose the self-consistency condition which is usually written in frequency space. Both the GF and the Weiss function contain the discontinuities at $\tau=0$ and $\tau=\beta$. The discontinuities in these functions and their derivatives determine the high-frequency behavior of their frequency-dependent Fourier transformations $G(\omega)$ and $G_0(\omega)$. As is well known, information about high-frequency behavior of GF's is absent in QMC simulations themselves (the maximum frequency available is the Nyquist frequency $\omega_{max}=1/2\Delta$, where Δ is the imaginary-time interval). The high-frequency (small imaginary-time) information is not contained in the QMC itself but has to be incorporated into the splining procedure using additional information.

This information is available from the calculation of corresponding moments of the GF's. To make this connection clear, we make a consecutive integration by parts of the Fourier integral:

$$G(i\omega_n)=\sum_{k=0}^{N}\frac{(-1)^{k+1}[G^{(k)}(0)+G^{(k)}(\beta)]}{(i\omega_n)^{k+1}}+\frac{(-1)^{N+1}}{(i\omega_n)^{N+1}}\int_0^\beta e^{i\omega_n\tau}\frac{\partial^{N+1}G(\tau)}{\partial\tau^{N+1}}d\tau. \quad \text{(A1)}$$

Values of the GF sum and its derivatives can be expressed via corresponding momenta. These momenta can be calculated similarly to the one-band Hubbard model.[17] A momentum of k degrees is defined as follows:

$$M^{(k)}=\int_{-\infty}^{+\infty}d\omega\omega^k\rho(\omega). \quad \text{(A2)}$$

We can bind Eqs. (A1) and (A2) by writing the following expression for the sum of GF's and its derivatives in imaginary-time space:

$$G^{(k)}(0)+G^{(k)}(\beta)=M^{(k)}, \quad \text{(A3)}$$

where $k=0\ldots N$. To make direct Fourier transformation, first, we interpolate $G(\tau)$ defined in L points (L is the number of time slices) and then take an analytical Fourier transformation of the resulting function. The procedure of interpolation plays a key role. We used the cubic spline interpolation for $G(\tau)$ where the condition of the continuous second derivative ($G^{(2)}$) is imposed. Using this condition we write a system of linear equations to find interpolation coefficients. To close the set of linear equations we need to set correct boundary conditions. The standard way to do this is to set the second derivatives at the end points of the time interval $[0,\beta]$ to zero (the so-called natural spline). In our approach we use analytical information about the momenta (the sum of the second and first derivatives at the end points, $M^{(1)}$ and $M^{(2)}$).

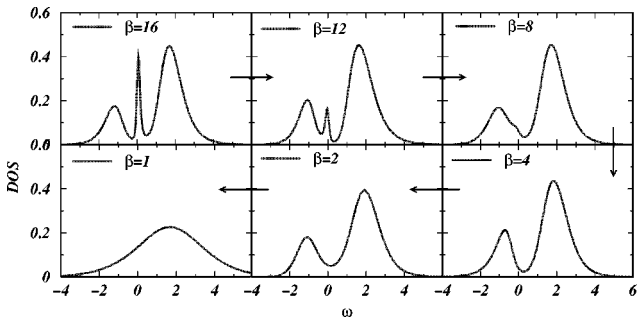

FIG. 5. Temperature dependence of the density of states for $U=3$.

To obtain this information we need to know the expansion of the self-energy in the $1/\omega$ series or in another words we need to know the first two momenta of the self-energy.

$$M_\Sigma^{(0)}=(2N-1)Un,$$

$$M_\Sigma^{(1)}=(2N-1)U^2n(1-(2N-1)n)+2U^2C_2^{2N-1}\langle nn\rangle, \quad \text{(A4)}$$

where N is the number of bands and $C_n^k=(k)!/n!(k-n)!$ is a combinatorial factor which arrives due to the spin and orbital degeneracies.

The self-energy expansion contains density-density correlation functions for different spins and orbitals. One way to obtain them is to use an approximate scheme which is accurate at high frequencies, such as the coherent-potential approximation.[18,19] Another possibility is to evaluate the correlation functions which enter in Eq. (A4) using the QMC procedure which allows us to compute arbitrary local correlation functions such as the density-density correlators. The self-consistency procedure ensures that they are correct cor-

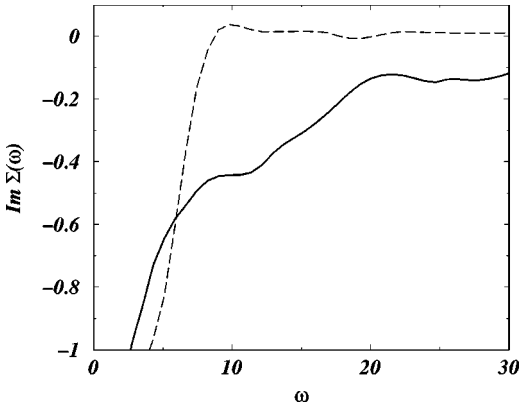

FIG. 6. Dependence of the imaginary part of the self-energy on the Matsubara frequency axis ω ($\beta=8$) for two different Fourier transformations, the "old" (dashed line) and the "new" (solid line).

relation functions when self-consistency is reached. Having correct momenta we solve the set of linear equations to obtain the cubic spline function which is Fourier-transformed analytically.

The power of modern computers allows us to use imaginary-time (τ) space up to $L=256$ time slices only, while in frequency (ω) space we do not have such limitations and can use as many frequency points as we want, but only frequencies less than the Nyquist frequency have physical meaning (usually less than 2^8). As we know, the GF has $1/\omega$ asymptotic behavior and dealing with the finite number of frequency points we introduce the finite-energy cutoff. Cutting off the tail of the GF, we remove the discontinuity from the Fourier-transformed function in τ space. To correct the situation we subtract the high-frequency tail from the GF and Fourier transform the obtained function numerically and the tail analytically. Finally, in τ space we sum up the obtained functions and as a result we have the correct inverse Fourier transformation; we call it the ''new'' one.

To demonstrate the difference between two ''old'' and ''new'' Fourier transformations we calculate the self-energy in the considered model for $U=4$ and $\beta=8$. Results are plotted in Fig. 6 where the ''new'' solution is drawn by a solid line and the ''old'' one is plotted by with dashed line. We see that the ''old'' one has the region where the self-energy changes sign (''overshoots''). It corresponds to an unphysical contribution to self-energy which should always keep the same sign for positive or negative frequencies. Finally, we stress that the difference between the two Fourier transformations becomes substantial especially in critical regions of parameters: low doping, high values of U, and low temperatures T.

*Permanent address: BLTPh, JINR, 141980 Dubna, Russia.

[1] G. Mahan, B. Sales, and J. Sharp, Phys. Today **50**, 42 (1997).
[2] G. Pálsson, V. S. Oudovenko, and G. Kotliar (unpublished).
[3] For a recent review, see, A. Georges, G. Kotliar, W. Krauth, and M. J. Rozenberg, Rev. Mod. Phys. **68**, 13 (1996).
[4] Th. Pruschke, D. L. Cox, and M. Jarrell, Phys. Rev. B **47**, 3553 (1993).
[5] M. J. Rozenberg, G. Kotliar, H. Kajueter, G. A. Thomas, D. H. Rapkine, J. M. Honig, and P. Metcalf, Phys. Rev. Lett. **75**, 105 (1995).
[6] J. Merino and R. H. McKenzie, Phys. Rev. B **61**, 7996 (2000).
[7] G. Pàlsson and G. Kotliar, Phys. Rev. Lett. **80**, 4775 (1998).
[8] H. Kajueter and G. Kotliar, Int. J. Mod. Phys. B **11**, 729 (1997).
[9] J. E. Hirsch and R. M. Fye, Phys. Rev. Lett. **56**, 2521 (1986); H. Q. Lin and J. E. Hirsch, Phys. Rev. B **37**, 1864 (1988).
[10] K. Takegahara, J. Phys. Soc. Jpn. **62**, 1736 (1992).
[11] Th. Pruschke, M. Jarrell, and J. Freericks, Adv. Phys. **44**, 187 (1995).
[12] H. Schweitzer and G. Czycholl, Phys. Rev. Lett. **67**, 3724 (1991).
[13] X. Yao, J. M. Honig, T. Hogan, C. Kannewurf, and J. Spalek, Phys. Rev. B **54**, 17 469 (1996).
[14] G. D. Mahan, *Many-Particle Physics*, 2nd ed. (Plenum, New York, 1993).
[15] P. Kwizera, M. S. Dresselhaus, and D. Adler, Phys. Rev. B **21**, 2328 (1980).
[16] A. K. Mabatah, E. J. Yoffa, P. C. Eklund, M. S. Dresselhaus, and D. Adler, Phys. Rev. Lett. **39**, 494 (1977).
[17] M. Potthoff, T. Wegner, and W. Nolting, Phys. Rev. B **55**, 16 132 (1997).
[18] B. Velicky, S. Kirkpatrick, and H. Ehrenreich, Phys. Rev. **175**, 747 (1968).
[19] H. Kajueter, Ph.D. thesis, Rutgers University, 1996.